Article ID: 1006-8775(2016) 02-0172-10

LINKAGE BETWEEN INDIAN OCEAN DIPOLE AND TWO TYPES OF El NIÑO AND ITS POSSIBLE MECHANISMS

DONG Di (董 笛)[1, 2], HE Jin-hai (何金海)[3], LI Jian-ping (李建平)[4, 5]

(1. State Key Laboratory of Numerical Modeling for Atmospheric Sciences and Geophysical Fluid Dynamics, Institute of Atmospheric Physics, Chinese Academy of Sciences, Beijing 100029 China; 2. College of Earth Science, University of Chinese Academy of Sciences, Beijing 100049 China; 3. Nanjing University of Information Science & Technology, Nanjing 210044 China; 4. College of Global Change and Earth System Science (GCESS), Beijing Normal University, Beijing 100875 China; 5. Joint Center for Global Change Studies, Beijing 100875 China)

Abstract: After compositing three representative ENSO indices, El Niño events have been divided into an eastern pattern (EP) and a central pattern (CP). By using EOF, correlation and composite analysis, the relationship and possible mechanisms between Indian Ocean Dipole (IOD) and two types of El Niño were investigated. IOD events, originating from Indo-Pacific scale air-sea interaction, are composed of two modes, which are associated with EP and CP El Niño respectively. The IOD mode related to EP El Niño events (named as IOD1) is strongest at the depth of 50 to 150 m along the equatorial Indian Ocean. Besides, it shows a quasi-symmetric distribution, stronger in the south of the Equator. The IOD mode associated with CP El Niño (named as IOD2) has strongest signal in tropical southern Indian Ocean surface. In terms of mechanisms, before EP El Niño peaks, anomalous Walker circulation produces strong anomalous easterlies in equatorial Indian Ocean, resulting in upwelling in the east, decreasing sea temperature there; a couple of anomalous anticyclones (stronger in the south) form off the Equator where warm water accumulates, and thus the IOD1 occurs. When CP El Niño develops, anomalous Walker circulation is weaker and shifts its center to the west, therefore anomalous easterlies in equatorial Indian Ocean is less strong. Besides, the anticyclone south of Sumatra strengthens, and the southerlies east of it bring cold water from higher latitudes and northerlies west of it bring warm water from lower latitudes to the 15° to 25°S zone. Meanwhile, there exists strong divergence in the east and convergence in the west part of tropical southern Indian Ocean, making sea temperature fall and rise separately. Therefore, IOD2 lies farther south.

Key words: Indian Ocean Dipole; two types of El Niño; anomalous Walker circulation; air-sea interaction; sea temperature anomaly

CLC number: P732 **Document code:** A

doi: 10.16555/j.1006-8775.2016.02.007

1 INTRODUCTION

As the most significant signal of global air-sea interaction, ENSO has been studied widely for a long period. However, since 1980s, El Niño events with initial warming in central equatorial Pacific Ocean have been noticed (known as dateline El Niño, see Larkin and Harrison [1], and El Niño Modoki, see Ashok et al.[2]). Kao and Yu [3] divided ENSO into two types based on previous studies: the Eastern-Pacific (EP) type and the Central-Pacific (CP) type. The two types of El Niño differ not only in formation mechanisms but also in their climatic effects. Similarly, sea temperature varies inter-annually in Indian Ocean as well. Saji et al.[4] found that the Indian Ocean Dipole (IOD) is with noticeable seasonal phase locking, usually develops in summer, and reaches its peak in autumn and decays rapidly in winter. Furthermore, Bahera and Yamagata [5] observed Subtropical Indian Ocean Dipole (SIOD), and pointed out that this is independent of IOD as it develops in winter and gets to its strongest phase in JFM the next year.

Many studies have investigated on the relationship between ENSO and IOD, whereas the heated debate lies in the independence of the two events. Some believed that they are distinctive of each other, IOD mainly results from Indian Ocean local air-sea interaction (Saji et al. [4]; Ashok et al. [6]; Webster et al. [7]), while others showed that the two events are in connection, including: (1) ENSO influences IOD: Nagura and Konda [8] found that the sea surface winds change direction in eastern equatorial Indian Ocean when El Niño begins, which affects the Indian Ocean SST. (2) IOD influences ENSO: Kug and Kang [9] argued that warming in the Indian Ocean, which is a part of the El Niño signal, operates as a negative feedback to ENSO. Wu and Kirtman [10] and

Received 2015-08-16; **Revised** 2015-12-02; **Accepted** 2016-04-15

Foundation item: National Key Basic Research Program of China (973 Program, 2012CB417403)

Biography: DONG Di, M.S., primarily undertaking research on air-sea interaction.

Corresponding author: HE Jin-hai, e-mail: hejhnew@nuist.edu.cn

Yu et al.[11] found that IOD has an impact on the intensity of ENSO by running GCM. (3) IOD and ENSO interact with each other: Annamalai et al.[12] pointed out that El Niño has been in a closer linkage with IOD since the Climate Shift; Wu and Meng [13] claimed that the gearing between the Indo monsoon circulation and the Pacific Walker circulation connects IOD and ENSO together.

Zhao et al.[14] found that the IOD event has two modes; one originates from tropical Indo-Pacific air-sea interaction, which is linked to ENSO, and the other is mainly from tropical Indian Ocean air-sea interaction, which is associated with the position and intensity of Mascarene High. Previous studies of the former IOD mode and ENSO's relationship were mostly based on the canonical ENSO type. However, with the CP El Niño identified, it is more concerned whether IOD has different connections with the two types of ENSO respectively. Moreover, previous studies mostly analyzed SST data, but Shinoda et al.[15] found that the IOD signal is more significant in the Indian Ocean subsurface, and it is also showed that SST anomaly in ENSO always originate from the thermocline of Pacific Western Pool (Chao[16]; Li[17]). Therefore, the sea temperature anomaly signal is often stronger at the thermocline, what about the Indian Ocean when IOD occurs? Does this have a linkage with ENSO? This paper tries to study these issues in order to help understand the relationship between IOD and ENSO.

2 DATA

The data used in this work include:

(1) Sea surface temperature (SST) monthly data are from Met Office Center on a 1°×1° mesh. The period selected is 1979–2012 for the reason that the data have been more reliable since 1950s and the discussion of Climate Shift influence is avoided;

(2) Sub-ocean temperature (SOT) data are based on World Ocean Database (WOD05) reanalysis with a 1°×1° resolution and non-isometric 13 layers in depth;

(3) Niño3, Niño4, IOD and SIOD indices are from NOAA;

(4) Wind field data are obtained from NCEP monthly reanalysis, on a mesh of 2.5°×2.5°.

3 CONTRASTING THE TWO TYPES OF EL NIÑO

As the SST patterns of two types of El Niño events are highly correlated, neither of the traditional Niño3 and Niño4 SST indices alone is effective in distinguishing them. In order to contrast the two types of ENSO in a better way, several indices have been proposed in recent years. In this paper, three representative indices are composited: (1) the first two modes of EOF analysis of tropical Pacific SSTA show EP and CP El Niño pattern respectively, the normalized time series of these two modes are used as the first representative index. (2) Though the time series of the first two EOF modes are orthogonal, the two types of ENSO cannot be regarded as completely separated events for they resemble in several ways. To compensate this, the second representative index N_{EP}, N_{CP} from Ren and Jin[18] are adopted:

$$\begin{cases} N_{EP}=N_3-\alpha N_4 \\ N_{CP}=N_4-\alpha N_3 \end{cases} \qquad \alpha=\begin{cases} 2/5 & N_3\cdot N_4>0 \\ 0 & N_3\cdot N_4\le 0 \end{cases}$$

Here, N_3 and N_4 denote Niño3 and Niño4 index respectively. (3) The two indices above are based on tropical Pacific SST anomalies, but the temperature anomaly maximum is often at the subsurface, the upper 100m's temperature anomalies are averaged over the eastern (80°–90°W, 5°S–5°N) and central (160°E–150°W, 5°S–5°N) equatorial Pacific to construct the two types of El Niño sub-ocean indices defined by Yu and Kao[19]. Afterwards, composite the three representative indices, normalize them and run three-months seasonal averaging, then, the composite EP and CP El Niño indices are obtained, as shown in Fig.1.

According to the two composite types of El Niño indices obtained, a strong El Niño event is selected when the index is over 1.5, and a weak El Niño is selected when the value is larger than 1.0 but less than 1.5. Therefore, the El Niño events in 1979–2012 are classified based on the above principle, results (shown in Table 1) are similar to that of Yu and Kao [19] and Ashok et al.[2].

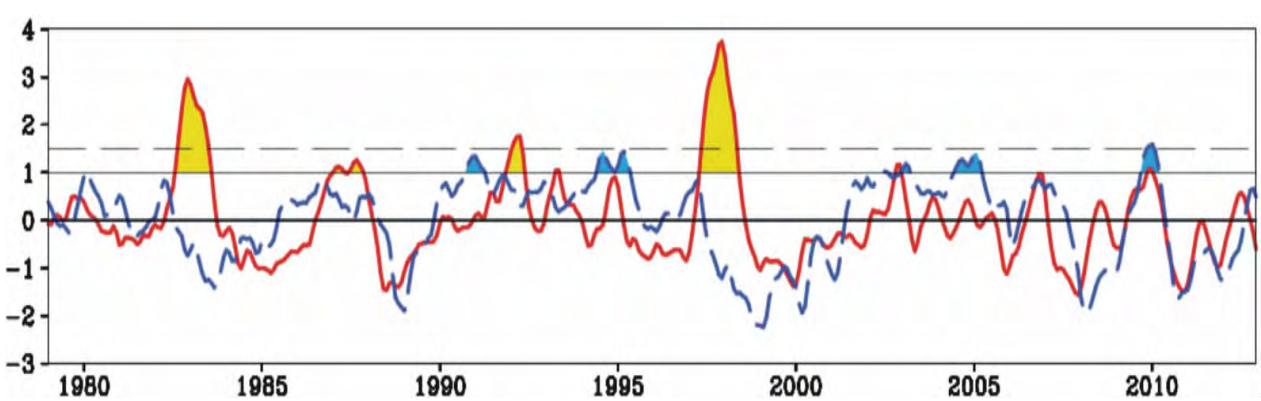

Figure 1. Composite EP El Niño index (red solid line) and CP El Niño index (blue dotted line).

Table 1. The classification of two-type El Niño according to the composite EP and CP indices.

El Niño type	EP El Niño	CP El Niño
Strong	1982/1983, 1991/1992, 1997/1998	2009/2010
Weak	1987/1988, 1992/1993, 2002/2003, 2009/2010	1979/1980, 1990/1991, 1994/1995, 2002/2003, 2004/2005

With the classifications in Table 1, the SSTA of Indian Ocean in boreal autumn (SON) and of tropical Pacific in the boreal winter (DJF) have been composited for a common picture of the two types of El Niño events. The result is remarkable, as illustrated in Fig.2.

During the boreal winter, the composite SSTA fields in tropical Pacific show a typical EP and CP El Niño respectively (Fig.2b and 2d), which confirms that the former indices defined can actually distinguish the two types of El Niño. Besides, when it comes to the Indian Ocean, a dipole structure, warmer in the western basin and cooler in the east, is found in both Fig.2a and 2c. However, it is noted that the location and intensity of the warmer and colder center are different in Fig.2a and 2c. This phenomenon will be explored in the following paper.

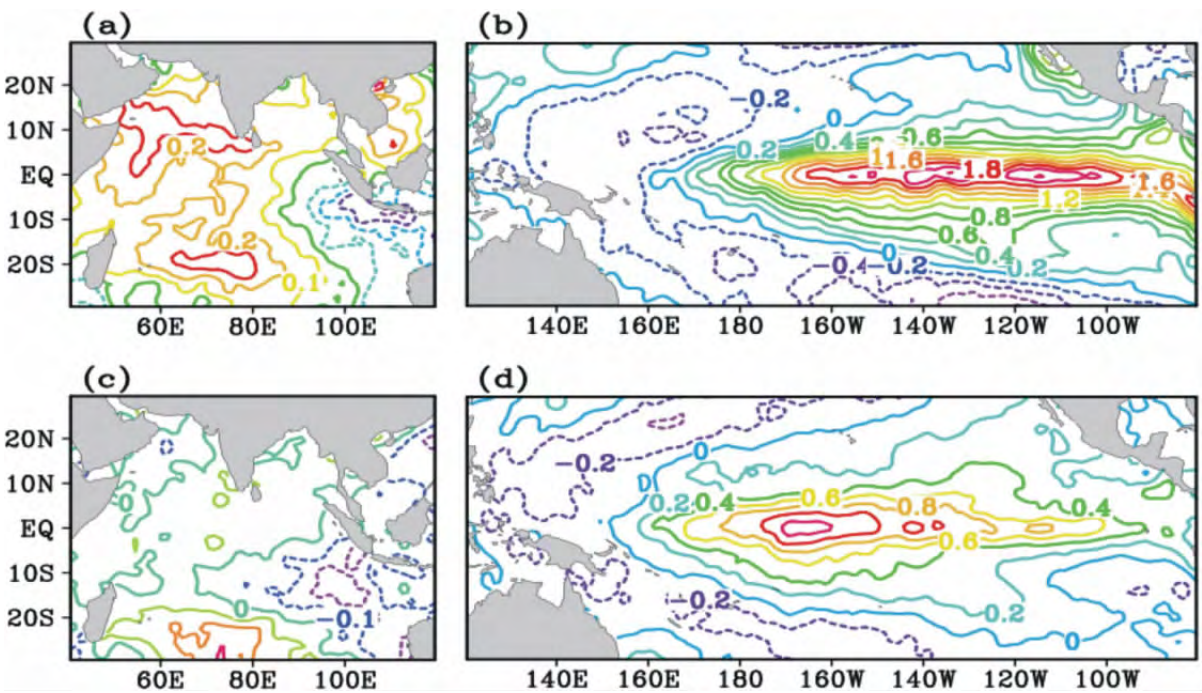

Figure 2. Composite Indian Ocean SSTA in autumn (SON) of EP (a) and CP (c) El Niño years; Composite tropical Pacific SSTA in winter (DJF) of EP (b) and CP (d) El Niño years.

4 IOD SSTA CORRESPONDING TO TWO TYPES OF EL NIÑO

The conventional IOD index, DMI (Dipole Mode Index [4]), is defined as the regional mean SSTA difference between eastern tropical Pacific (50°–70°E, 10°S–10°N) and south-eastern tropical Indian Ocean (90°–110°E, 0°–10°S). The correlation coefficients of DMI vs. Niño 3 index and DMI vs. Niño 4 index are 0.38 and 0.27 respectively. Due to this weak correlation, Saji, Ashok and some scientists believed that IOD is incited mainly by local air-sea interaction in the Indian Ocean while ENSO has little influence on it. However, it is worth noticing that as the Niño 3 index contains signals of both types of El Niño, will the correlation get stronger when we study the IOD with the two types of El Niño individually?

To visualize the sub-ocean temperature anomaly in the Indian Ocean, correlation between the two types of composite El Niño indices defined and equatorial Indian Ocean (10°S–10°N) 0–400 m mean SOTA is shown in Fig.3. From Fig.3a, an overall positive anomaly is found in the sea surface layer, but the warmer layer is very shallow in the east while quite deep in the west. It is the shallow eastern warmer anomalies that make the Indian Ocean surface dipole signal less significant. However, as it is going deeper, the sub-ocean dipole mode is very strong, which reaches its maximum around 50–150 m. Hence, the DMI calculated from the Indian Ocean SSTA does not characterize IOD as well as that based on SOTA. On the other hand, Fig.3b indicates that an anomalous warm center is in the upper sea level of the

Indian Ocean when CP El Niño occurs. In this case, however, the sub-ocean layer does not show a dipole mode as in Fig.3a, instead, it is mainly colder than usual.

According to the analyses above, the equatorial Indian Ocean Dipole is more significant at the sub-ocean layer and bears a closer relationship with EP El Niño than with CP El Niño. To further illustrate this, an EOF method is adopted on the SSTA and mean SOTA (0–400 m) respectively, with the leading EOF modes in the two cases shown in Fig.4.

From the Indian Ocean SSTA EOF1 mode (Fig. 4a), the basin-wide warming is the leading mode in the Indian Ocean SST anomaly while no dipole mode is observed. Besides, the correlation coefficient in Fig.4b between EOF1 time series and composite EP index is 0.4, but a three-month lagged correlation is 0.58, indicating that this basin-wide warming lags El Niño by about three months, generally known as Indian Ocean Basin-wide Warming (IOBW) which develops in winter and peaks in spring. This is beyond the discussion here. On the other hand, Fig. 4c shows a very clear IOD SSTA distribution in which the anomalous cold temperature extends westwards off Sumatra like a tongue, the warmer part has a "<" shape distribution, both warmer and colder anomalies are symmetric about the equator and

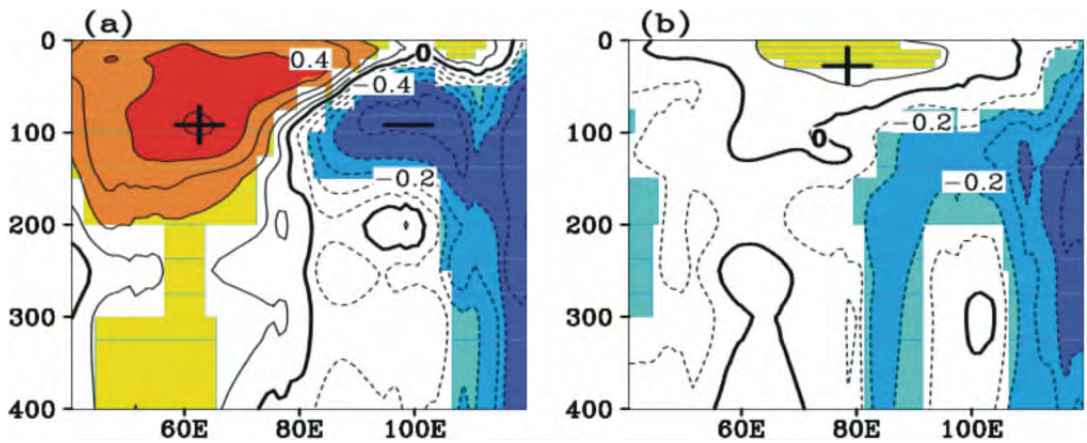

Figure 3. Longitude-depth correlation coefficients of mean equatorial Indian Ocean (10°S–10°N) SOTA with composite EP index (a), CP index (b). Significant values over 95% confidence level from a two-tailed Student's *t*-test are shown in shades.

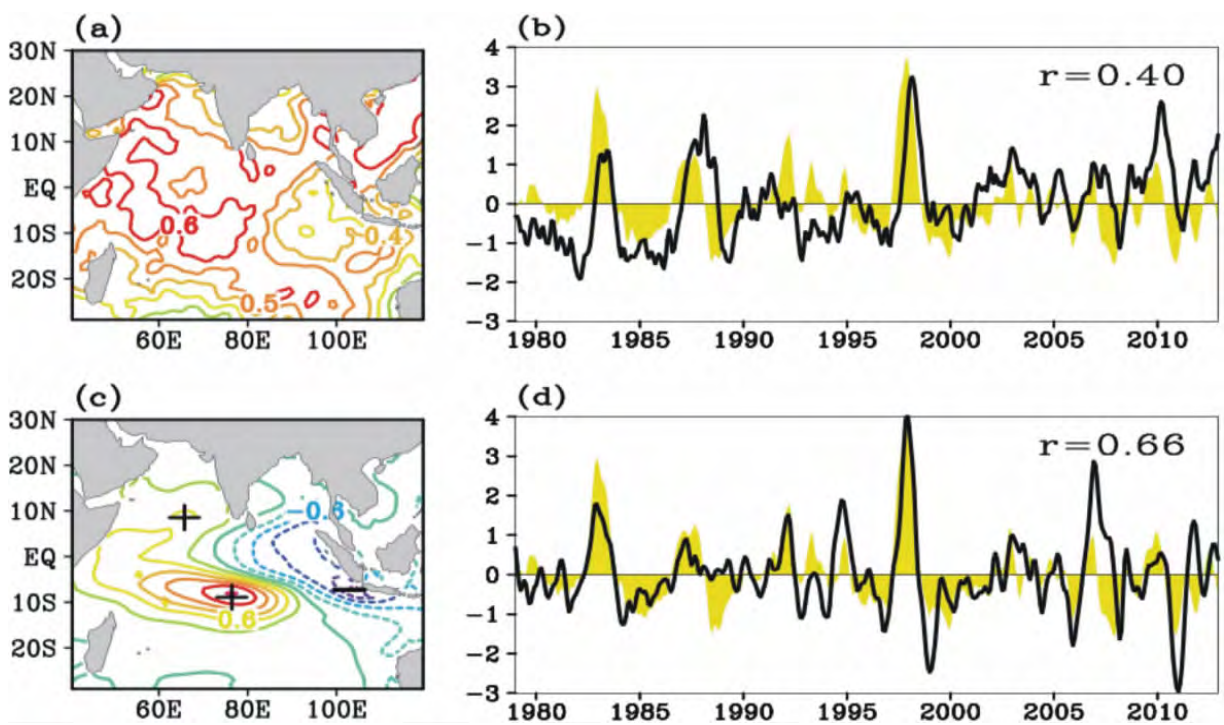

Figure 4. The first EOF mode and normalized time series of SSTA (a, b) and 0-150 m mean SOTA (c, d) in Indian Ocean. The two EOF1 contribute 32.4% and 30.0% respectively. In b and d, solid line is EOF time series and yellow shadow denotes composite EP index, r denotes correlation between the composite EP index and EOF time series.

stronger in the south. In Fig. 4d, the SOTA EOF1 time series correlates with the composite EP index by up to 0.66 but only 0.23 with the composite CP index. Therefore, the equatorial Indian Ocean dipole signal is more significant at the sub-ocean layer of 0–150 m, and it is more closely related to the EP El Niño.

In contrast, Fig.3b shows that the IOD signal related to CP El Niño is not quite significant, and the correlation coefficient between DMI and composite CP index is only 0.23. Does it indicate that IOD is independent of CP El Niño events? However, Fig.2c illustrates that a composite east-cold west-warm dipole mode is still in coexistence with the CP El Niño. What features does this kind of IOD have? To explore it, the correlation between the composite CP index and the Indian Ocean SSTA is determined and the result is shown in Fig.5. In this case, the dipole mode in the Indian Ocean is observed with a negative center in the sea northwest of Australia and a positive center in tropical southern Indian Ocean at 60°–80°E. Furthermore, Fig.5b illustrates longitude-depth correlation coefficient distribution of composite CP index and mean SOTA of tropical southern Indian Ocean. Compared with Fig.3b, the dipole mode is easily found at the upper layer of tropical southern Indian Ocean. Based on this, the dipole mode related to CP El Niño probably occurs in the 15°–25°S tropical part of south Indian Ocean.

In order to investigate the aforementioned conjecture, the EOF of Indian Ocean monthly SSTA is done, with the second leading mode EOF2 shown in Fig.6. From EOF2, the dipole mode mainly occurs in the tropical southern Indian Ocean's upper layer instead of the equatorial Indian Ocean. This agrees with that in Fig.2c and Fig.5a. In the meantime, the EOF2 time series correlates with the composite CP index by up to 0.48 but only 0.23 with the composite EP index. All the analyses indicated that tropical southern Indian Ocean dipole lies father south and relates to CP El Niño more closely.

Above analyses indicated that the IOD modes related to the two types of El Niño differ in several aspects like strength and location: the IOD mode associated with the canonical EP El Niño is more significant at the sub-ocean of equatorial Indian Ocean and shows a quasi-symmetric distribution, stronger in the south, about the equator. Here, we call it IOD1 for convenience. On the other hand, the IOD mode associated with the CP El Niño stands out in the tropical southern Indian Ocean upper layer, named as IOD2. In order to distinguish these two IOD modes, two indices are calculated based on IOD1 and IOD2's location. Similar to re-

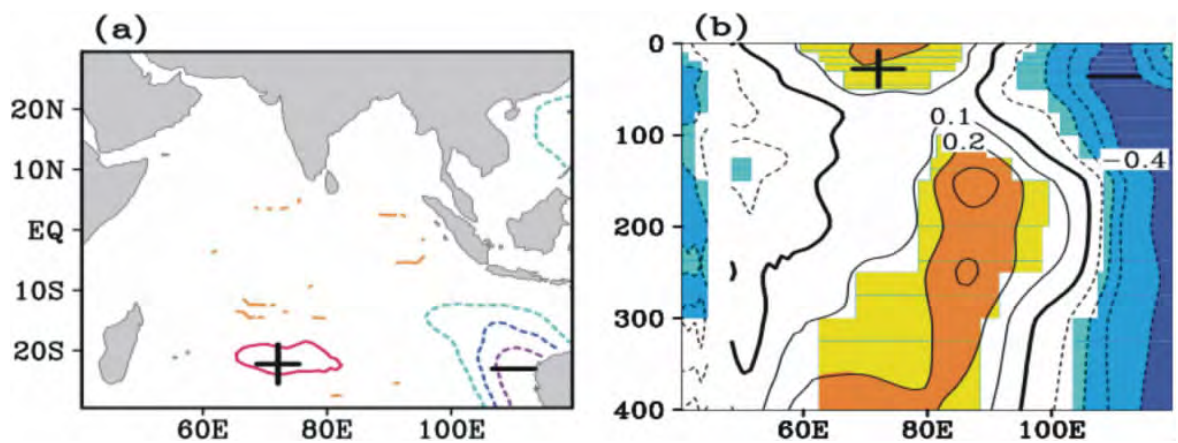

Figure 5. Correlation between composite CP indices (a) with values significant over the 95% confidence level shown; the longitude-depth correlations coefficients between composite CP indices and tropical southern Indian Ocean (15°–25°E) mean SOTA (b) with values over the 95% confidence level in shades.

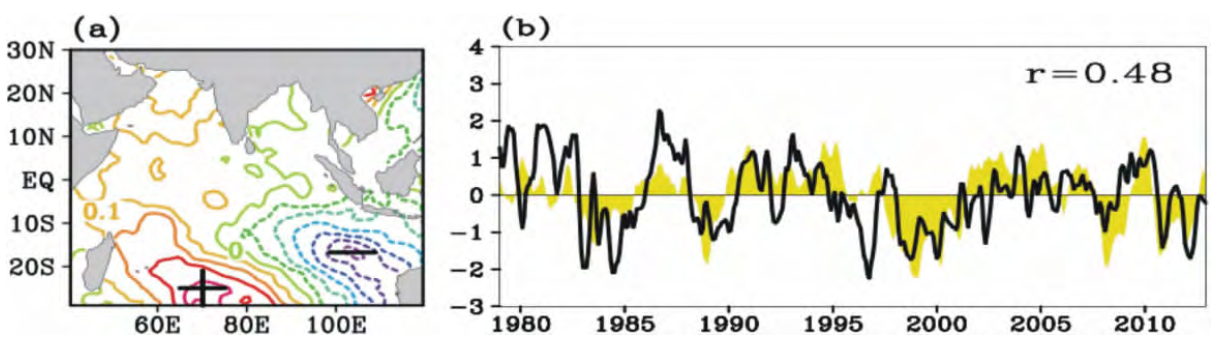

Figure 6. EOF2 of Indian Ocean monthly SSTA (a); solid line in (b) denotes EOF2 time series and yellow shade denote composite CP index, correlation between them is 0.48.

gions in DMI, the IOD1 index is defined as a normalized 0 to 150 m mean SOTA difference between equatorial western (50°–70°E, 10°S–10°E) and eastern (90°–110°E, 0°–10°S) Indian Ocean, shown in Fig.7a together with a composite EP index and the correlation between them is as high as 0.65. The IOD2 index is defined as a normalized mean SSTA difference between tropical south-western (60° –80° E, 15° –25° S) and south-eastern (100°–120°E, 15°–25°S) Indian Ocean. The IOD2 and composite CP index, as shown in Fig.7b, correlate by up to 0.60. The high correlation coefficients indicate that the two types of El Niño and IOD's relationship can be investigated more clearly when the IOD mode is divided into two kinds. However, it is noticeable that IOD2 here is not the same kind of SIOD (Subtropical Indian Ocean Dipole) by Bahera and Yamagata[5] for the SIOD index bears little correlation with the IOD2 index. Last but not least, these two IOD modes are not completely separated as they associate and sometimes overlap each other, thus, some years witness the IOD mode with both the IOD1 and IOD2 features at the same time like 1992 and 1993.

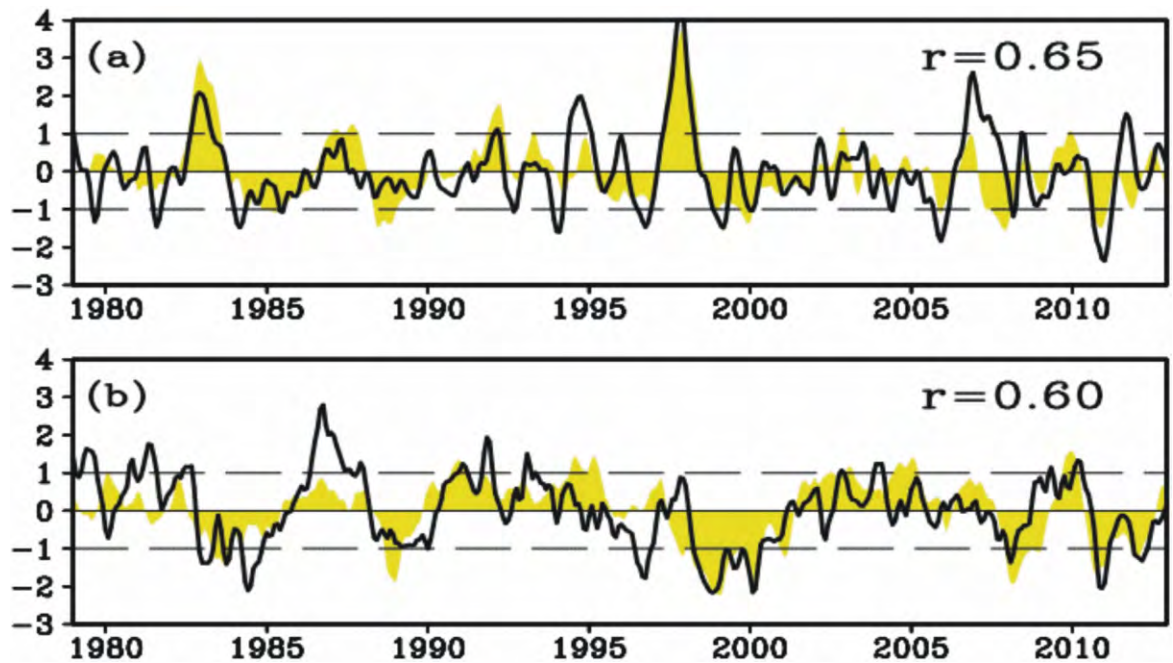

Figure 7. Solid line in (a) and (b) is normalized IOD1 and IOD2 index respectively; yellow shade in (a) and (b) is composite EP and CP index respectively; r is the correlation coefficient.

5 INVESTIGATION OF THE MECHANISMS LINKING IOD AND THE TWO TYPES OF EL NIÑO

The spatio-temporal links between sea surface temperatures and winds reveal a strong coupling [4] between them. During dipole mode events, the sea surface wind field over the tropical Indian Ocean experiences large changes, especially in its zonal (east-to-west) component over the Equator. To investigate the zonal wind stress before EP and CP El Niño reach their mature phases, 1000-hPa mean zonal wind anomalies of corresponding autumns (SON) are composited in equatorial Indian Ocean and Pacific, and the results are shown in Fig.8a. Besides, a three-month lagged correlation is computed between the two composite ENSO indexes and the 1000-hPa zonal wind anomalies, shown in Fig.8b and 8c. From Fig.8, in an earlier stage before EP El Niño peaks, relatively strong anomalous west wind above the equatorial Pacific and anomalous east wind above the equatorial Indian Ocean start to blow. The opposite direction of wind anomalies in the equatorial Indian and Pacific Oceans is associated with the strong coupling between the monsoonal zonal circulation over the equatorial Indian Ocean and the Walker circulation over the Pacific Ocean [13]. From Fig. 8b, the downdraft of Walker circulation related to EP El Niño is located around 130°E. The west wind anomaly is centered at the central equatorial Pacific while the east wind anomaly center is over Sumatra, both relatively strong. Hence, the strong east wind anomalies off Sumatra force the upwelling in situ, shoaling the thermocline, decreasing the subsurface temperature in east equatorial Indian Ocean where IOD1 occurs.

In contrast, when focusing on the wind anomalies before CP El Niño peaks, it is found that the downward branch of Walker circulation moves to 110°E, the west and east wind anomalies are both relatively weak. The 1000-hPa maximum west wind anomaly center lies more westward compared to that in Fig.8b and the min-

imum center lies south off Sumatra. Therefore, as the cold upwelling is forced by a relatively weak east wind stress, it is not so intense so that the sea temperature there does not decrease much.

In summary, combined with the sea temperature anomalies of IOD1 and IOD2, a general air-sea interaction mechanism can be pictured. When EP El Niño starts, the anomalous Walker circulation is relatively strong, there is significant east wind anomaly off Sumatra in Indian Ocean, dragging sea water to the west. As warmer water is accumulating in the west Indian Ocean and deep colder water keeps ascending in the east, a dipole mode is formed both at surface and subsurface due to the strong dynamic air-sea interaction. On the other hand, when CP El Niño occurs, the Walker circulation is relatively weak, and lies more west. The east wind anomaly is relatively weak, thus the dragging force is not so strong, and there's no significant dipole mode in equatorial Indian Ocean when CP El Niño occurs.

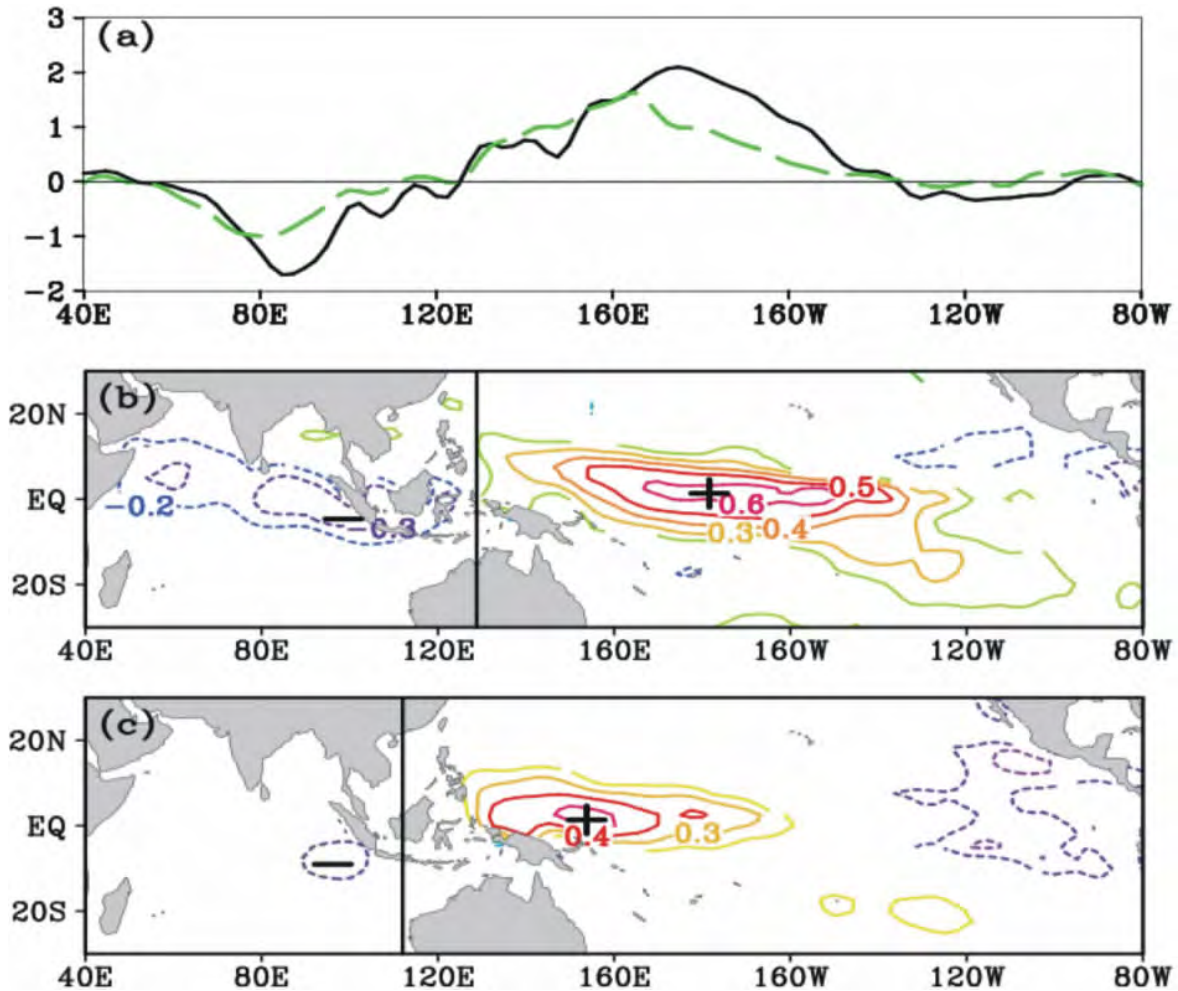

Figure 8. (a) EP (solid line) and CP (dotted line) El Niño autumn (SON) 1 000-hPa zonal wind stress anomalies in equatorial Indian-Pacific Ocean (5°S-5°N). (b) and (c) are three-month lagged correlations between composite EP, CP index and 1 000-hPa zonal wind anomalies respectively, with values over 95% confidence shown.

The explanations above focus on the zonal wind anomalies and are applicable to the formation of IOD1. However, if we go further, some questions may be asked: Why does IOD1 have a sea temperature distribution like a "<" shape, and why is it stronger in the south? As IOD2, which is associated with CP El Niño, occurs, why is there no significant temperature anomaly along the equator though east wind anomalies still exist in the Indian Ocean?

In the analysis of zonal wind anomalies here in this work, the wind circulation is considered due to its importance in forcing sea water motion. The cyclone (anticyclone) in the Northern Hemisphere (NH) can force the divergence (convergence) of the upper-layer sea water which shoal (deepen) the thermocline layer, as a result, the temperature of sea upper layer will decrease (increase), and the opposite is true in the Southern Hemisphere (SH). The correlations between two defined IOD indices and 1000-hPa wind stress anomalies and wind vorticity anomalies are shown in Fig.9.

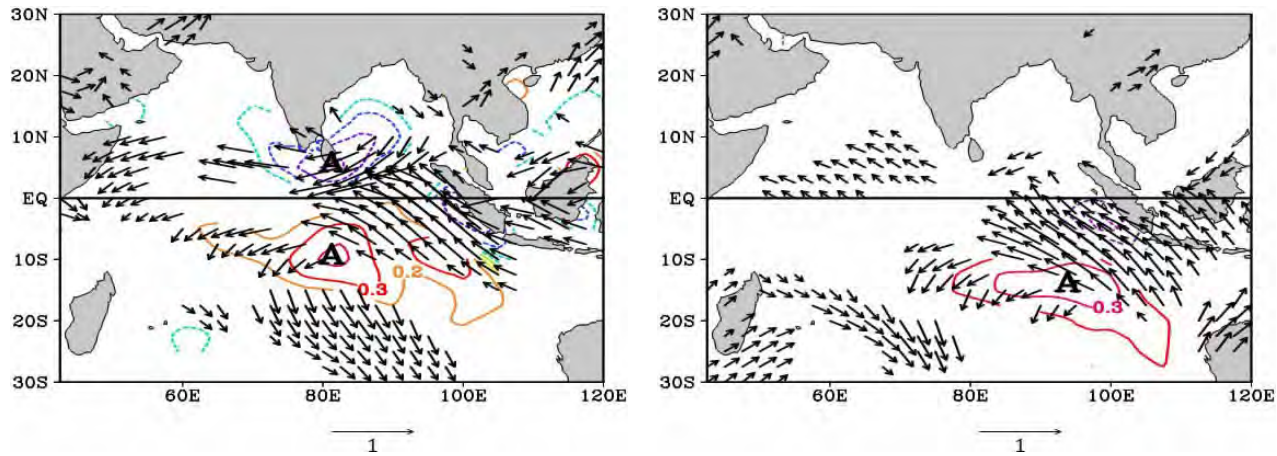

Figure 9. Correlations between IOD1 (a), IOD2 (b) and 1 000-hPa sea surface wind stress anomalies (shown in arrows) and wind vorticity anomalies (shown in contours), with values over 95% confidence level drawn.

Figure 9a illustrates that when IOD1 occurs, there are two anomalous anticyclones, symmetric about the equator along 80°E. The location and intensity of these two anticyclones are in correspondence with the two warm centers of IOD1 in Fig.4c. Because of these two anticyclones, the north-easterlies from the NH and south-easterlies from SH converge in the eastern equatorial Indian Ocean, dragging sea water westward, and making cold water ascend in the east and warm water accumulate in the west. Due to the strong wind stress anomalies, the upwelling is also intense, leading to marked east-to-west IOD signals at the upper layer of equatorial Indian Ocean. Furthermore, the two anticyclones here also contribute to the western warming due to their divergence effect, and warm water accumulate in the anti-cyclonic centers. It is notable that the anticyclone in SH is more intense and its warming effect is also more significant, as a consequence, the warm center in the south of IOD1 is stronger. Therefore, these two anticyclones account for why IOD1 has a "<" like warming distribution that is stronger in the south.

In the contrary, when IOD2 occurs, the northern anomalous anticyclone is unobservable while the southern anomalous anticyclone is still quite significant with its position moved to further east. The moderate northern anticyclone weakens the north-easterly anomalies in the NH, causing the eastern equatorial Indian Ocean wind convergence to decrease in intensity; in the meantime, the warm water accumulates at the center of the anomalous anticyclone in the SH, deepening the thermocline. Due to the combined mechanisms, the upwelling in the east and westward dragging effect become weak, and there is no significant dipole SSTA in the equatorial Indian Ocean. As mentioned above, however, there is a dipole mode, IOD2, in the southern tropical Indian Ocean around 15°–25°S. For the anticyclone in the SH (as in Fig.9b), the southerlies to its east edge bring cold water from high latitudes to low latitudes along the west coast of Australia, and at the same time, the divergent wind anomalies force upwelling in the sea west of Australia, and consequently, the combined effects lead to the cold center in the north-west sea of Australia. Similarly, to the west of this anticyclone, the anomalous northerlies bring warmer water in the equatorial zone to higher latitudes, wind anomalies converge in 60°–80°E of the tropical southern Indian Ocean, resulting in deeper thermocline and warmer sea temperature there. However, since the wind anomalies are rather weak in IOD2 events, the dipole mode is confined mainly in the sea-surface layer of tropical south Indian Ocean.

Based on the previous analyses, the anomalous sea-surface wind plays an important role in influencing IOD which links to the two types of El Niño mainly in three aspects: (1) the dragging of equatorial anomalous easterlies, (2) the forcing of anticyclones, and (3) the forcing of wind anomalous divergence and convergence effect. A question may be raised: Do these three effects bear the same importance?

To inquire into this issue, several measurements are defined to represent different effects. The mean zonal wind anomalies of eastern equatorial Indian Ocean (80°–100°E, 10°S–10°N) is defined to measure eastern equatorial Indian Ocean zonal wind intensity (named as equatorial eastern zonal wind). For IOD1 events, the 1000-hPa mean vorticity anomalies of region 80°–100°E, 5°–15°N and of region 80°–100°E, 5°–15°S are defined to measure north equatorial anticyclone intensity (anticyclone north of equator) and south equatorial anticyclone intensity (anticyclone south of equator) respectively; for IOD2 events, the 1000-hPa mean wind vorticity anomalies of region 90°–110°E, 10°–20°S are defined to measure the strength of the anticyclone south of Sumatra (anticyclone south of Sumatra). Finally, to evaluate the divergence effects in tropical southern Indian Ocean, the mean wind divergence anomalies of the

regions (100°–120°E, 15°–25°N) and (60°–80°E, 20°–30°N) are calculated (named as divergence east and divergence west) to measure the wind divergence anomalies in the east and west part of tropical south Indian Ocean respectively. The correlations between the two IOD indices and the six measurements in the regions concerned are shown in Table 2. The results show that the IOD1 index correlating with equatorial eastern zonal wind anomalies is the most significant, up to –0.78, this means that the dragging effect of equatorial zonal wind in the eastern Indian Ocean is the most important factor that generates the IOD1 event. The IOD1 index with the anticyclones on the two sides of the equator is also quite high, indicating that these two anticyclones contribute to IOD1 as well, especially in shaping the warmer anomalies of IOD1.

The IOD2 index has a 0.4 correlation coefficient with zonal wind, and this means that the zonal wind along the equator in IOD2 is not as strong as in IOD1 and the zonal wind forcing is relatively weak. However, the IOD2 index has relatively high correlation with the intensity of the anticyclone south of Sumatra. Therefore, with the moderate zonal wind and the effect of the anticyclone south of Sumatra, cold SSTA is not as significant in the equatorial eastern Indian Ocean as in the sea west of Australia. In addition, the IOD2 index also has a relatively high correlation with the divergence and convergence in the tropical southern Indian Ocean, which contributes to IOD2's formation.

Table 2. Correlations between two IOD indices and the six measurements in the concerned regions.

	IOD1 index	IOD2 index
Equatorial eastern zonal wind	–0.78	–0.40
Anticyclone north of equator	0.63	0.24
Anticyclone south of equator	0.46	0.25
Anticyclone south of Sumatra	0.43	0.55
Divergence east	0.20	0.55
Divergence west	–0.28	–0.42

6 CONCLUSIONS AND DISCUSSIONS

By compositing three representative ENSO indices, El Niño events have been selected and divided into EP and CP type. By using EOF, correlation and composite analysis, the relationship and possible mechanisms be tween IOD and the two types of El Niño events have been investigated.

(1) The Indian Ocean dipole events related to El Niño can be divided into two kinds: one is associated with EP El Niño and has strongest signal at 50–150 m in the equatorial Indian Ocean sub-surface layer, symmetric about the equator but stronger in the south; the other one is more closely related to CP El Niño events and is significant between 15°–25°S in tropical southern Indian Ocean.

(2) Two IOD indices have been defined according to their temperature anomalies location. The IOD1 index is based on the mean SOTA of equatorial Indian Ocean, and it has a high correlation (0.68) with composite the EP El Niño index; while the IOD2 index is based upon SSTA of tropical southern Indian Ocean and has a high correlation (0.60) with the CP El Niño index.

(3) IOD1 is strongly dependent on the anomalous east wind along the equatorial Indian ocean and the anomalous anticyclones on the two sides of the equator. In the developing phase of EP El Niño, the anomalous downward branch of Walker circulation is around 130°E, strong anomalous zonal easterlies start to blow, dragging sea water westward. The sea surface anomalous wind forcing cold water upwelling and warm water accumulating is the main mechanism causing the IOD1 mode. Besides, the anticyclones on the two sides of the equator deepen the thermocline layer in central-western equatorial Indian Ocean and make the sea temperature rise. As the southern anticyclone is stronger, its warming effect is more significant.

(4) IOD2 is mainly dependent on the anomalous anticyclone south of Sumatra and divergence effect in the tropical Southern Indian Ocean. When CP El Niño develops, the anomalous Walker circulation sinks down at 110°E, further west and weaker compared to the EP El Niño. The anomalous east wind weakens and the cooling effect thus decreases. However, the anomalous anticyclone south of Sumatra intensifies and has two effects: on the one hand, the warming effect in the center of the anticyclone weakens the upwelling in the east equatorial Indian Ocean; on the other, the southerlies to the east of it bring cold water and northerlies to the west to bring warm water into zone of 15°–25°S. In addition to the relatively strong divergence in the east and convergence in the west of tropical south Indian Ocean, IOD2 occurs mainly in the latitude of 15°–25°S, more southward than IOD1.

The Indo-Pacific air-sea interaction has an important impact on IOD events though the local effect cannot be neglected. This paper investigated the possible dynamic mechanisms, mainly on wind anomalies, which links the two types of El Niño and IOD events. More mechanisms and the local effect should be discussed in

the next stage of our study.

REFERENCES:

[1] LARKIN N K, HARRISON D E. Global seasonal temperature and precipitation anomalies during El Niño autumn and winter [J]. Geophys Res Lett, 2005, 32 (16): L16705, doi:10.1029/2005GL022860.

[2] ASHOK K, BEHERA S K, RAO S A, et al. El Niño Modoki and its possible teleconnections [J]. J Geophys Res, 2007, 112: C11007, doi:10.1029/2006JC003798.

[3] KAO H Y, YU J Y. Contrasting eastern-Pacific and central-Pacific types of ENSO [J]. J Climate, 2009, 22 (3): 615-632.

[4] SAJI N H, GOSWAMI B N, VINAYANDRANCHAN P N, et al. A dipole in the tropical Indian Ocean [J]. Nature, 1999, 401(23): 360-363.

[5] BAHERA S K, YAMAGATA T. Subtropical SST dipole events in the Southern Indian Ocean [J]. Geophys Res Lett, 2001, 28(2): 327-330.

[6] ASHOK K , GUAN Z Y, YAMAGATA T, et al. A Look at the Relationship between the ENSO and the Indian Ocean Dipole [J]. J Meteorol Soc Jpn, 2003, 81(1): 41-56.

[7] WEBSTER P J, MOORE A M, LOSCHNIGG J P, et al. Coupled ocean-atmosphere dynamics in the Indian Ocean during 1997-98 [J]. Nature, 1999, 401(6751): 356-360.

[8] NAGURA M, KONDA M. The seasonal development of an SST anomaly in the Indian Ocean and its relationship to ENSO [J]. J Climate, 2007, 20(1): 38-52.

[9] KUG J S, KANG I S. Interactive Feedback between ENSO and the Indian Ocean [J]. J Climate, 2006, 19(9): 1 784-1 801.

[10] WU R, KIRTMAN B P. Understanding the Impacts of the Indian Ocean on ENSO variability in a coupled GCM [J]. J Climate, 2004, 17(20): 4 019-4 031.

[11] YU J Y, CARLOS R. MECHOSO, et al. Impacts of the Indian Ocean on the ENSO cycle [J]. Geophys Res Lett, 2002, 29(8): 1204, doi:10.1029/2001GL014098.

[12] ANNAMALAI H, XIE S P, MCCREARY J P. Impact of Indian Ocean sea surface temperature on developing El Niño [J]. J Climate, 2005, 18(2): 302-319.

[13] WU Guo-xiong, MENG Wen. Gearing between the Indo monsoon Circulation and the Pacific Walker Circulation and the ENSO [J]. Chin J Atmos Sci, 1998, 22 (4): 470-480 (in Chinese).

[14] ZHAO Yong-ping, CHEN Yong-li, Wang fan, et al. Two modes of tropical Indian Ocean Dipole [J]. Sci China (Earth Sci), 2008, 38(10): 1 318-1 328 (in Chinese).

[15] SHINODA T, HENDON H H, ALEXANDER M A, et al. Surface and subsurface dipole variability in the Indian Ocean and its relation with ENSO [J]. Deep-Sea Res I, 2004, 51: 619-635.

[16] CHAO Ji-ping. New understanding of the development of El Niño and La Niña [J]. Bull Chin Acad Sci, 2001, 6: 412-417.

[17] LI Chong-yin. Further study of essence of El Niño [J]. Clim Environ Res, 2002, 7(2): 160-174.

[18] REN H L, JIN F F. Niño indices for two types of ENSO [J]. Geophys Res Lett, 2011, 38: L04704, doi: 10.1029/2010GL046031.

[19] YU J Y, KAO H Y. Subsurface ocean temperature indices for Central-Pacific and Eastern-Pacific types of El Niño and La Niña events [J]. Theor Appl Climateol, 2011, 103: 337-344.

Citation: DONG Di, HE Jin-hai and LI Jian-ping. Linkage between Indian Ocean Dipole and two types of El Niño and its possible mechanisms [J]. J Trop Meteorol, 2016, 22(2): 172-181.